

## Fully integrated design of a stretchable kirigami-inspired micro-sized zinc-sulfur battery

Ahmad Amiri <sup>a</sup>, Kian Bashandeh <sup>a</sup>, Ronald Sellers <sup>a</sup>, Louis Vaught <sup>a</sup>, Mohammad Naraghi <sup>b</sup>,  
and Andreas A. Polycarpou <sup>a,\*</sup>

<sup>a</sup> J. Mike Walker '66 Mechanical Engineering Department, Texas A&M University, College  
Station, TX, USA

<sup>b</sup> Department of Aerospace Engineering, Texas A&M University, College Station, Texas  
77843, USA

\* E-mail: [apolycarpou@tamu.edu](mailto:apolycarpou@tamu.edu)

### Mechanical and electrochemical characterization

An Instron 5543 single column table top tensile tester with 1 kN load cell was utilized to measure the mechanical properties of the stretchable kirigami-inspired Zn-S battery. All the electrochemical tests were conducted by a CH Instrument 660E Bipotentiostat. For non-linear discharge curves, specific capacitance was calculated by equation S1. The capacitance ( $C_{sp}$ ), capacity ( $Q$ ), and efficiency ( $\eta$ ) were obtained by applying Eqs. (S1), (S2), and (S3).

$$C_{sp} = \frac{2 i \cdot A \cdot t_d}{m_{act} \cdot \Delta V^2} \quad (S1)$$

$$Q = t_d(s) \frac{i}{3.6 m_{act}} \quad (S2)$$

$$\text{Efficiency} = \frac{t_d}{t_c} \times 100 \quad (S3)$$

The energy density ( $E$ ) and power density ( $P$ ) were respectively calculated by questions S4 and S5 <sup>[1]</sup>.

$$E = \left( \frac{C_{sp}}{7.2} \right) (\Delta V)^2 \text{ (mWh/g)} \quad (S4)$$

$$P = 3600 \cdot E / \Delta t \text{ (mW/g)} \quad (S5)$$

In the equations,  $i$  is the current,  $m_{act}$  is the cumulative masses of the anode and cathode electrodes,  $t_d$  is the discharge time,  $t_c$  is the charge time,  $\Delta V$  is the scanning potential window and

A is the electrode surface area. Energy and power densities were calculated based on the total mass of the cathode material.

## Tables

*Table S1. Discharge and charge reactions in the stretchable Zn-S battery*

Discharge Reactions	$S + Zn^{2+} + 2e^- \rightarrow ZnS$ $S + Zn^{2+} + I_2 + 4e^- \rightarrow ZnS + 2I^-$ $I^- + I_2 \rightarrow I_3^-$
Charge Reactions	$ZnS \rightarrow S + Zn^{2+} + 2e^-$ $2ZnS + 4H_2O \rightarrow S + 2Zn^{2+} + SO_4^{2-} + 8H^+ + 10e^-$ $ZnS + I_3^- \rightarrow S + Zn^{2+} + 1.5 I_2 + 3e^-$ $2ZnS + 4H_2O + I_3^- \rightarrow S + 2Zn^{2+} + SO_4^{2-} + 1.5 I_2 + 8H^+ + 11e^-$

*Table S2. Nitrogen adsorption (BET) results of porous CNFs*

	BET surface area m <sup>2</sup> /g	Average pore diameter (nm)	Total pore volume cm <sup>3</sup> /g
KOH-treated AC (AC)	1241.634	2.38	0.7391
AC-S	2.948	13.40	0.009876
As-received AC	467.55	2.31	0.27

*Table S3. Nitrogen adsorption (BET) results of porous CNFs*

Energy storage type	Configuration	Stretchability [%]	Gravimetric, areal and volumetric energy density	Reference
Crumpled Graphene Supercapacitor	2D planar	140	–	[2]
Graphene Supercapacitor	3D-Textile	140	–	[3]
Carbon nanotubes – fabric Supercapacitor	3D -Textile	220	20 Wh/kg	[4]
Manganese dioxide- Carbon nanotubes Supercapacitor	3D -Textile	220	2.6 ×10 <sup>-3</sup> mWh/cm <sup>2</sup>	[5]
Polypyrrole-fabric Supercapacitor	3D -Textile	200	11.1 Wh/kg	[6]
Polypyrrole /reduced graphene oxide fabric Supercapacitor	3D -Textile	150	2.53 Wh/kg	[7]
Manganese dioxide nanowires Supercapacitor	3D - Kirigami	600	21.07×10 <sup>-3</sup> mWh/cm <sup>2</sup>	[8]

Carbon nanotubes Supercapacitor	3D - Textile	130	20 Wh/kg	[9]
Polypyrrole-Carbon nanotubes Supercapacitor	3D -Textile	180	61.3 $\mu\text{Wh}/\text{cm}^2$	[10]
Carbon nanotubes Supercapacitor	3D -Textile	150	–	[11]
Graphite-cellular paper Supercapacitor	3D -Origami	130	–	[12]
Graphene-decorated Metallic textile Supercapacitor	3D -Textile	290	$6.1 \times 10^{-3}$ Wh/ $\text{cm}^3$	[13]
Graphene Supercapacitor	3D -Kirigami	382.5	–	[14]
Polypyrrole-Manganese dioxide-Carbon nanotubes Supercapacitor	3D -Textile	121	31.1 Wh/kg	[15]
Zn-MnO <sub>2</sub>	Fiber-like	300	447 mWh g <sup>-1</sup> (98.5 % retention after 500 cycles)	[16]
Zn-Ag	2D planar	100	3.93 mWh cm <sup>-2</sup> (140 % after 30 cycles at 100 % strain)	[17]
Li-ion Batteries	Origami	1300	0.53 mWh cm <sup>-2</sup>	[18]
Li-ion Batteries	2D planar	50	8.14 mWh cm <sup>-2</sup> (85 % after 60 cycles)	[19]
Li-ion Batteries	Fiber-like	600	201 mWh g <sup>-1</sup> (90 %, after 50 cycles)	[20]
Li-ion Batteries	Fiber-like	100	345 mWh g <sup>-1</sup> (84 % after 200 cycles)	[21]
Li-ion Batteries	Fiber-like	100	231 mWh g <sup>-1</sup> (92.1 % after 100 cycles)	[22]
Li-air	Serpentine	100	2540 Wh kg <sup>-1</sup>	[23]
Al-air	Fiber-like	30	935 mA h g <sup>-1</sup>	[24]
Na-ion battery	3D -Textile	50	278 mWh g <sup>-1</sup> (85 % after 60 cycles)	[25]
Zinc-sulfur battery	Kirigami	200	184.8 mWh/g (19.6 % increase after 10,000 stretch/release cycles under 200% under 200% tensile strain)	This study
Zinc-sulfur battery	Kirigami	200	184.8 mWh/g (6.3 % drop after 10,000 stretch/bending cycles of 200% strain and 180° bending angle)	This study

*Table S4. AC impedance equivalent circuit fitting parameters*

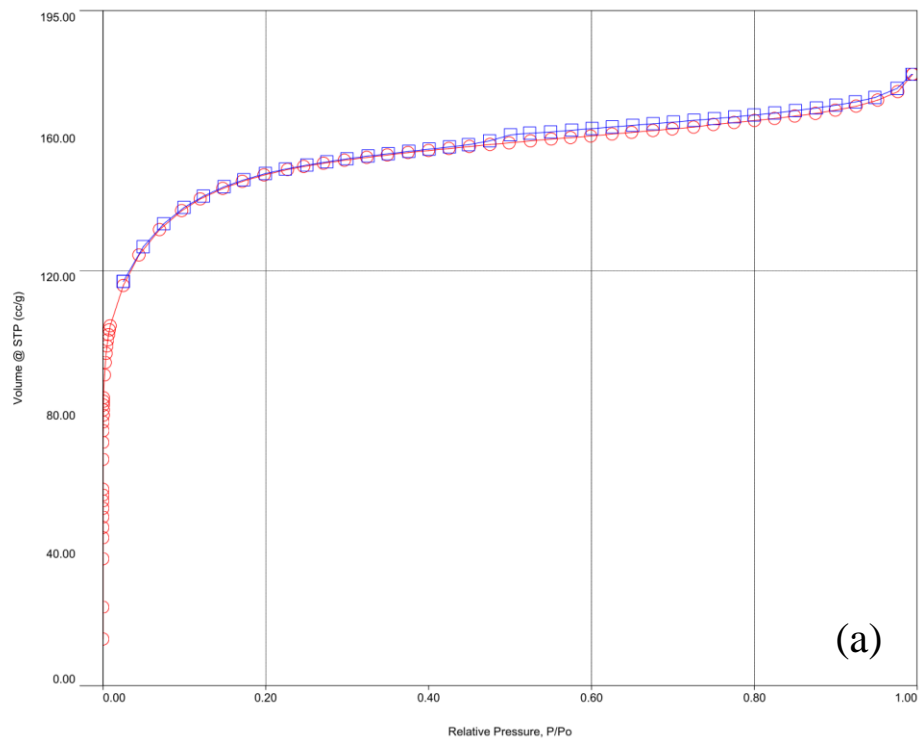
	<b>R<sub>s</sub> (Ω)</b>	<b>R<sub>i</sub></b>	<b>R<sub>ct</sub></b>	<b>W</b>
0% strain and 1 <sup>st</sup> cycle	7.28	6.27	12.81	0.03
50% strain and 1 <sup>st</sup> cycle	7.12	5.80	11.55	0.03
100% strain and 1 <sup>st</sup> cycle	7.86	5.39	9.7	0.03

150% strain and 1 <sup>st</sup> cycle	6.71	5.15	9.80	0.03
200% strain and 1 <sup>st</sup> cycle	6.09	2.64	6.02	0.03
0 % strain and 800 <sup>th</sup> cycle	14.16	10.15	23.32	0.01
200 % strain and 800 <sup>th</sup> cycle	13.88	9.52	18.63	0.01

Table S5. AC impedance equivalent circuit fitting parameters

	$R_s$ ( $\Omega$ )	$R_i$	$R_{ct}$	$W$
0% strain and 1 <sup>st</sup> cycle at -25 °C	22.2	24.39	13.46	0.03
0% strain and 1 <sup>st</sup> cycle at -25 °C	23.24	23.27	13.84	0.03

## Figures



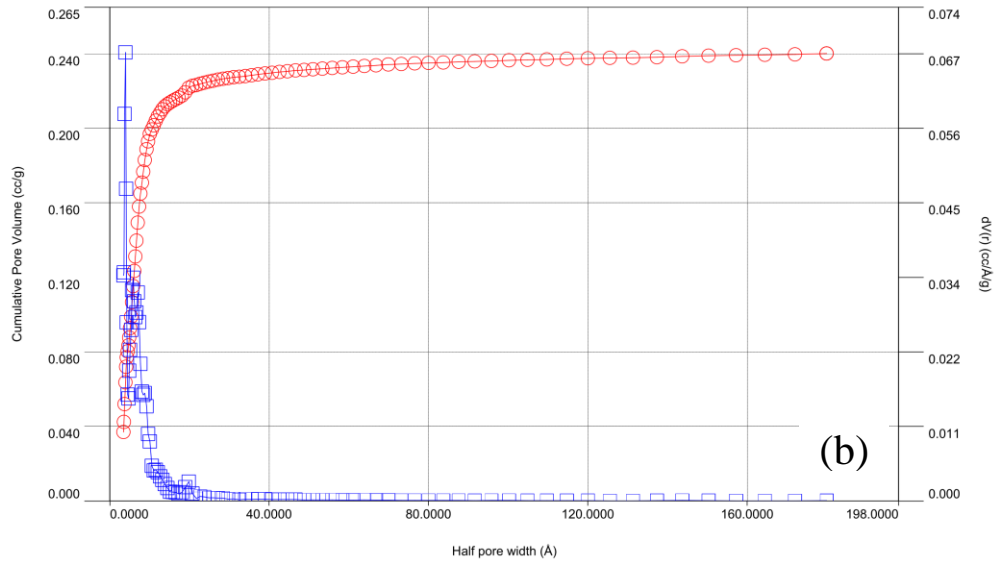


Fig. S1. (a) Adsorption-desorption isotherms and (b) distribution of pore size of as-received AC.

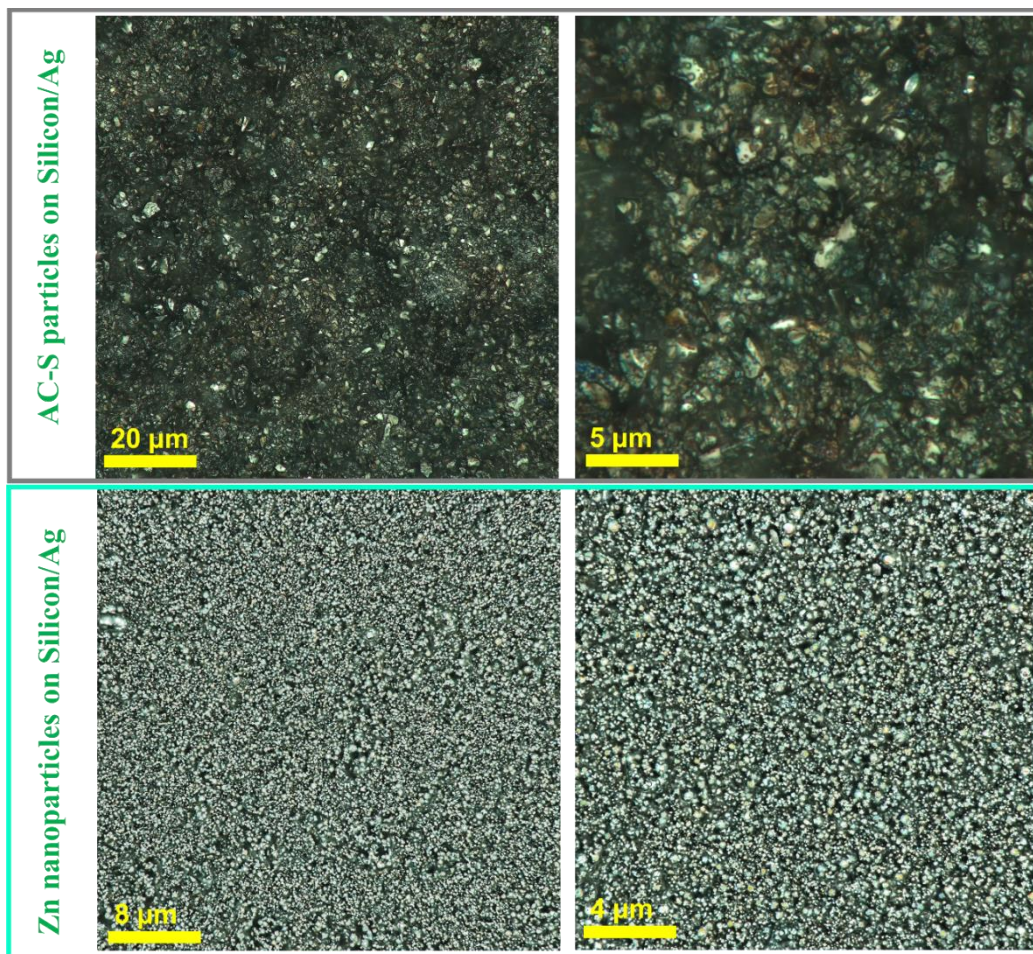


Fig. S2. The optical images of AC-S and zinc nanoparticles distributed on the current collector.

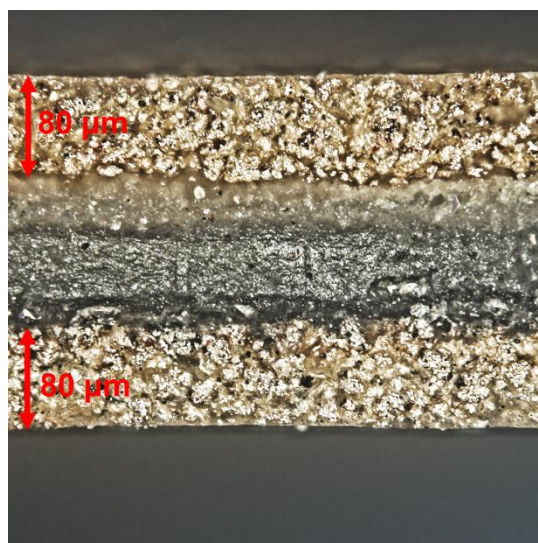
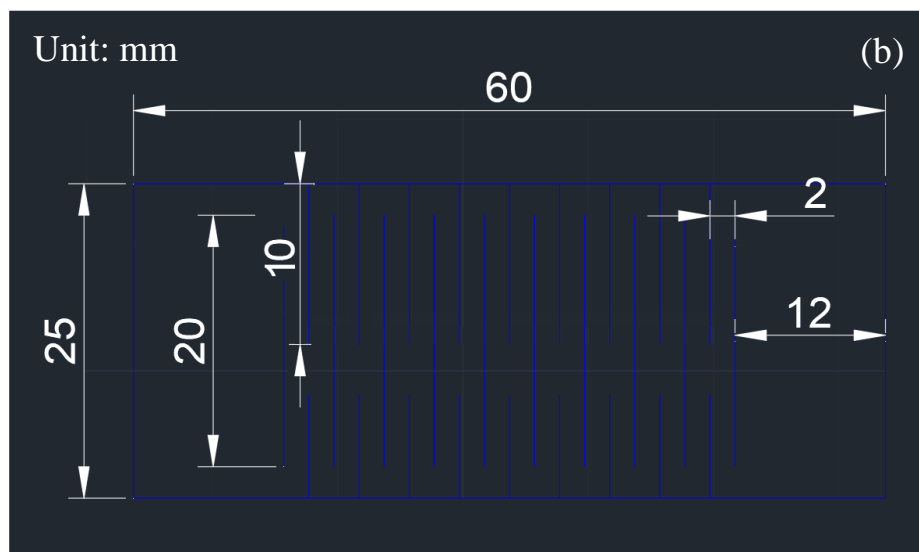
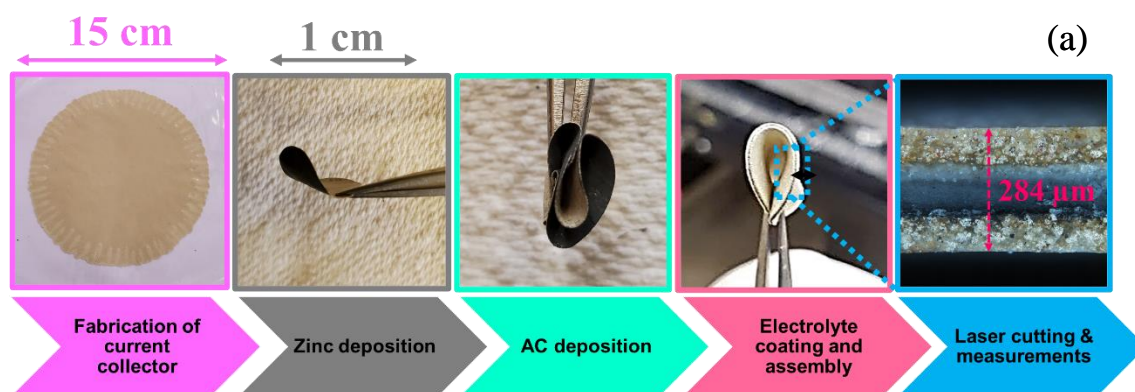


Fig. S3. The optical images of kirigami- inspired Zn-S cell. The thin film of cured silver-filled silicone adhesive possessed an average thickness of  $80 \pm 20 \mu\text{m}$ .



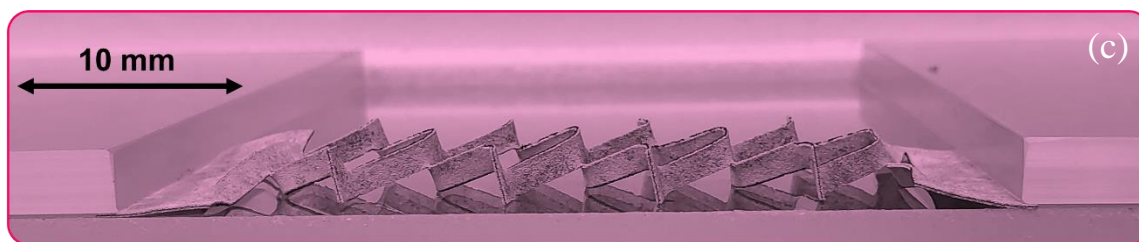


Fig. S4. (a) The photographs of the stretchable kirigami-inspired Zn-S battery in different stages of fabrication. (b) Dimensions and patterns for laser cutting. (c) 3D structure of the kirigami-inspired Zn-S battery.

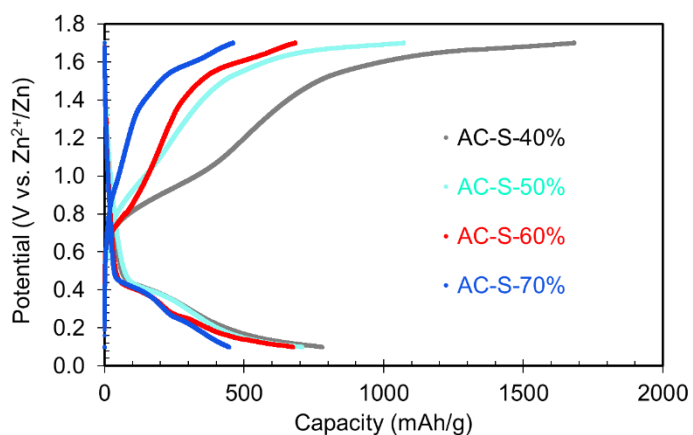


Fig. S5. Charge and discharge profiles of Zn-S battery for samples with different sulfur contents at 0.25 A/g.

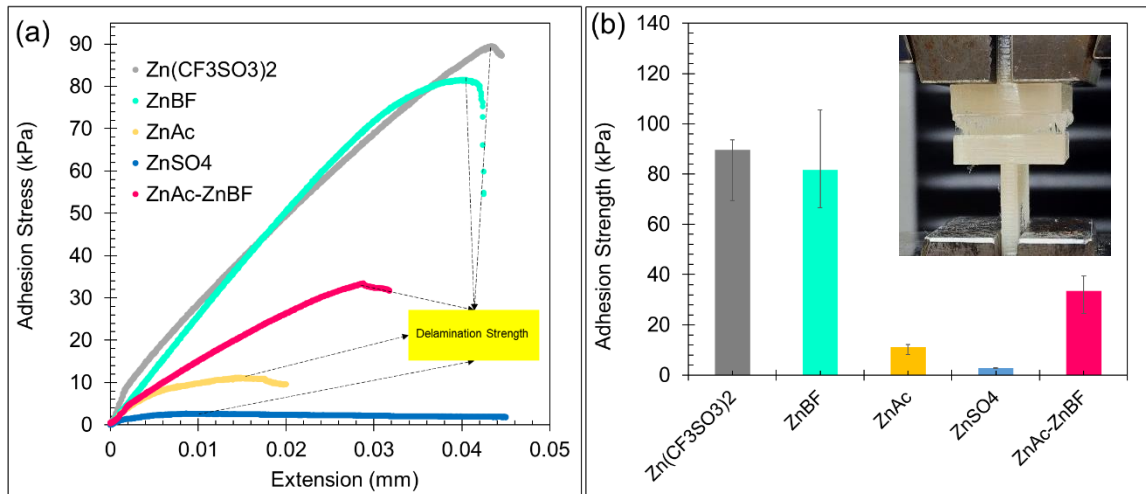


Fig. S6. (a) Typical stress–extension plots and (b) adhesion strength of different zinc salt-containing hydrogels.

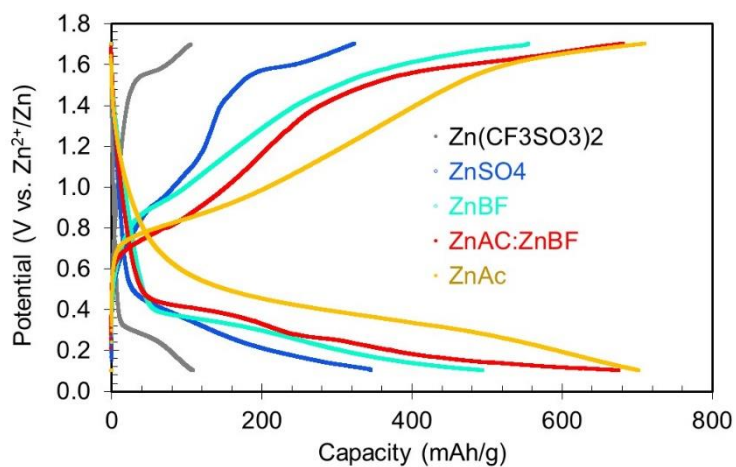


Fig. S7. Charge and discharge profiles of Zn-S battery in the presence of different electrolytes at 0.25 A/g.



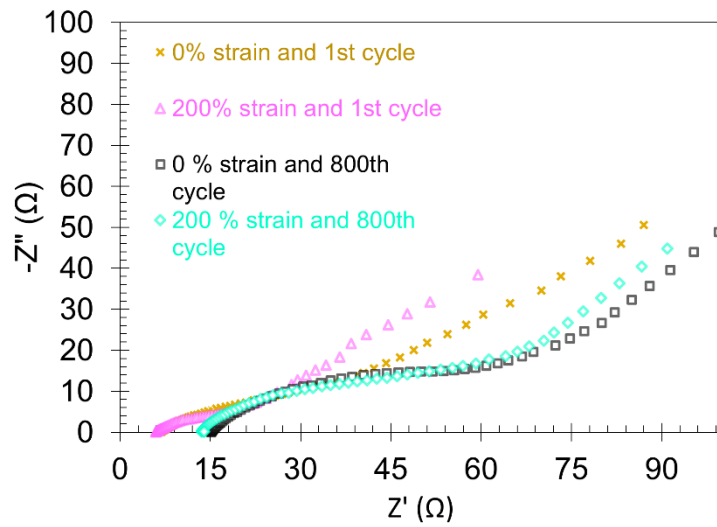
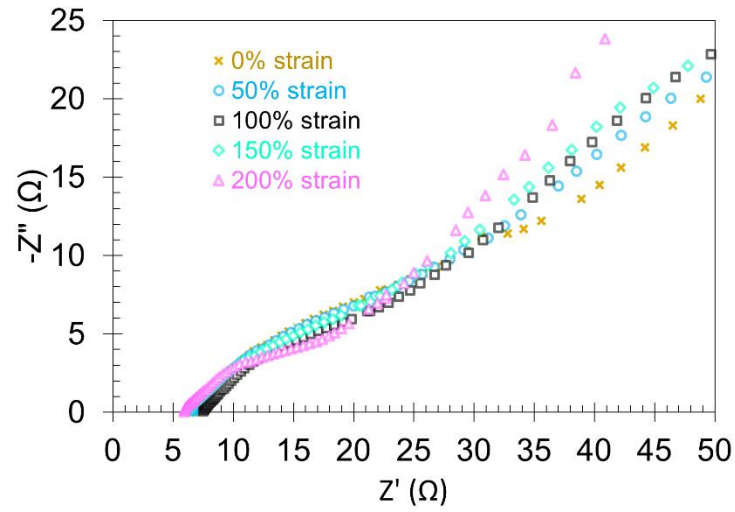


Fig. S8. Nyquist plots of kirigami-inspired Zn-S battery as a function of (a) strain and (b) cycle.

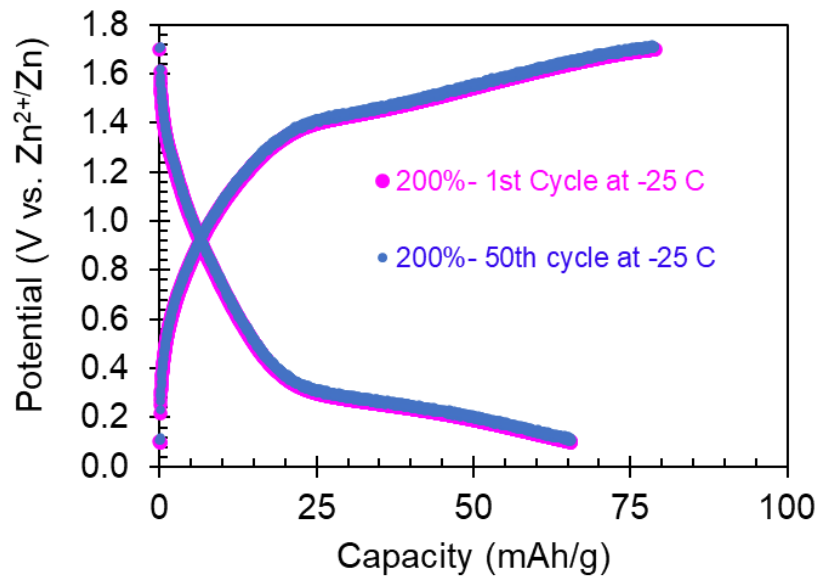


Fig. S9. Charge and discharge profiles of the kirigami-inspired Zn-S battery subjected to 1 and 50 stretching cycles under 200% tensile strain at -25 °C.

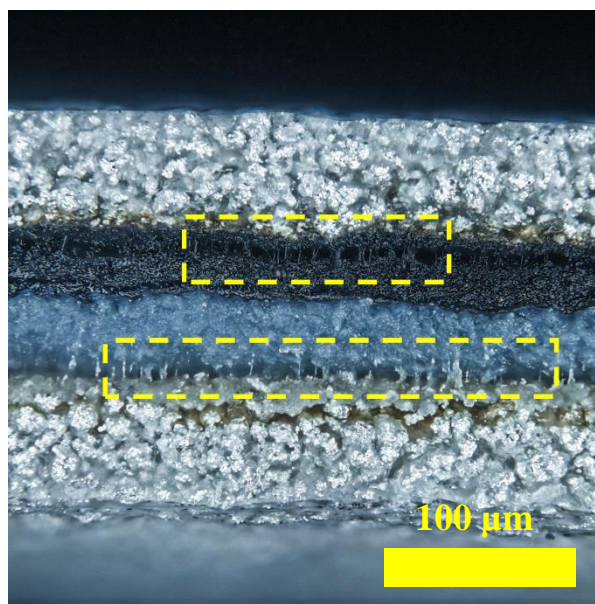


Fig. S10. The optical image of the partial delamination between electrodes and current collector at -25 °C. We observed a handful of delaminated sites only at -25 °C.

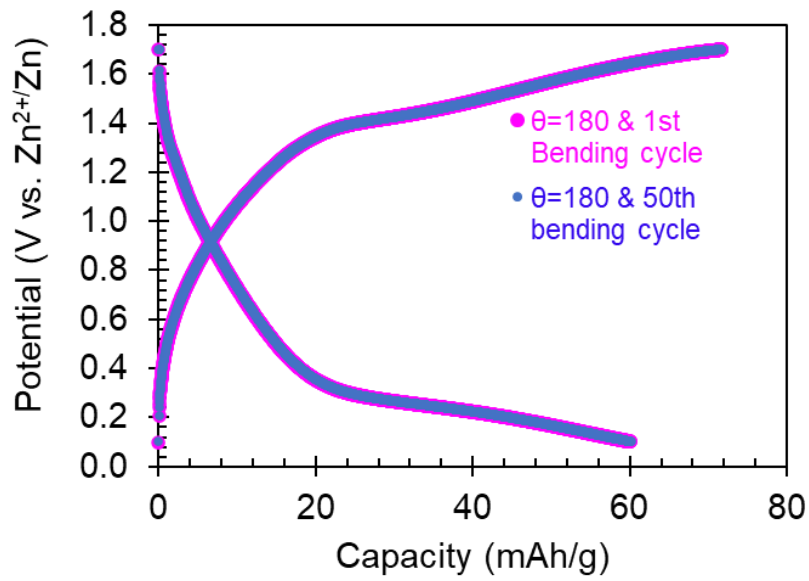


Fig. S11. Charge and discharge profiles of the kirigami-inspired Zn-S battery subjected to 1 and 50 bending cycles under 180° at -25 °C.

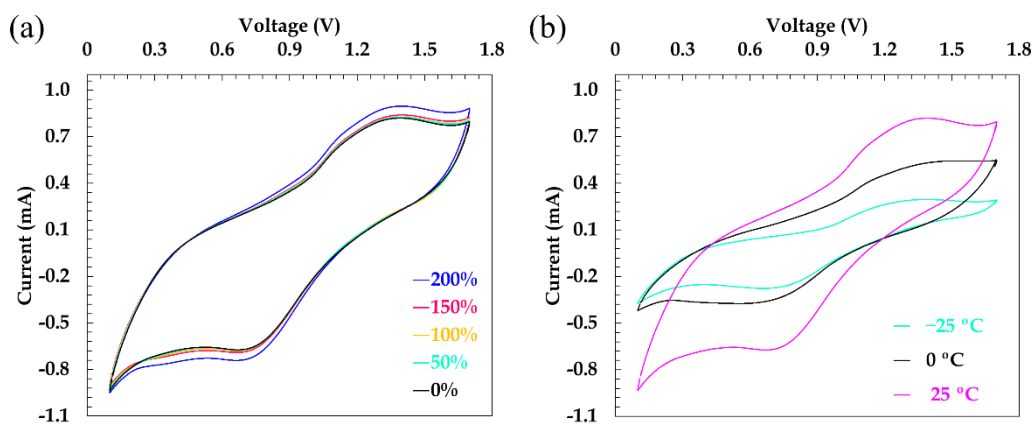


Fig. S12. CV charts of the kirigami-inspired Zn-S battery as a function of (a) tensile strain at 25 °C and 1 mV/s and (b) temperature at 1 mV/s.

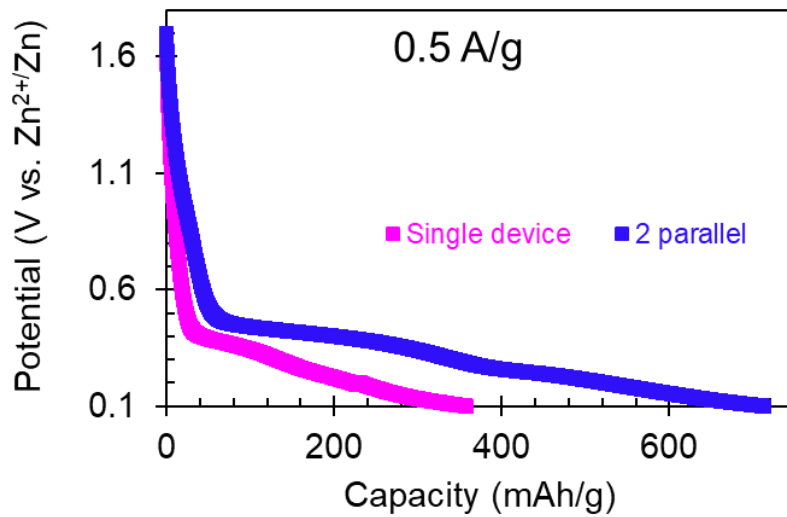


Fig. 13. Discharge curves of two Zn-S assembled in a parallel design vs. a single device at 0.5 A/g.

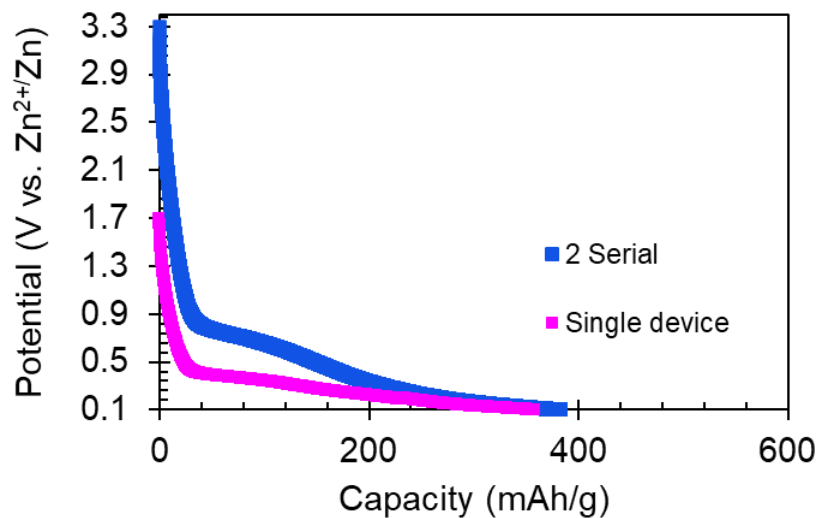


Fig. 14. Discharge curves of two Zn-S assembled in a serial design vs. a single device at 0.5 A/g.

## References

- [1] S. C. Sekhar, G. Nagaraju, J. S. Yu, Nano Energy 2017, 36, 58; Q. Meng, K. Qin, L. Ma, C. He, E. Liu, F. He, C. Shi, Q. Li, J. Li, N. Zhao, ACS applied materials & interfaces 2017, 9, 30832; G. Lee, S. K. Kang, S. M. Won, P. Gutruf, Y. R. Jeong, J. Koo, S. S. Lee, J. A. Rogers, J. S. Ha, Advanced Energy Materials 2017, 7, 1700157.

- [2] T. Chen, Y. Xue, A. K. Roy, L. Dai, ACS nano 2014, 8, 1039.
- [3] X. Zang, M. Zhu, X. Li, X. Li, Z. Zhen, J. Lao, K. Wang, F. Kang, B. Wei, H. Zhu, Nano Energy 2015, 15, 83.
- [4] L. Hu, M. Pasta, F. La Mantia, L. Cui, S. Jeong, H. D. Deshazer, J. W. Choi, S. M. Han, Y. Cui, Nano letters 2010, 10, 708.
- [5] C. Choi, S. H. Kim, H. J. Sim, J. A. Lee, A. Y. Choi, Y. T. Kim, X. Lepró, G. M. Spinks, R. H. Baughman, S. J. Kim, Scientific reports 2015, 5, 1.
- [6] B. Yue, C. Wang, X. Ding, G. G. Wallace, Electrochimica Acta 2012, 68, 18.
- [7] C. Zhao, K. Shu, C. Wang, S. Gambhir, G. G. Wallace, Electrochimica Acta 2015, 172, 12.
- [8] Z. Lv, Y. Luo, Y. Tang, J. Wei, Z. Zhu, X. Zhou, W. Li, Y. Zeng, W. Zhang, Y. Zhang, Advanced Materials 2018, 30, 1870008.
- [9] D. Kim, G. Shin, Y. J. Kang, W. Kim, J. S. Ha, Acs Nano 2013, 7, 7975.
- [10] J. Sun, Y. Huang, C. Fu, Z. Wang, Y. Huang, M. Zhu, C. Zhi, H. Hu, Nano Energy 2016, 27, 230.
- [11] Y.-H. Lee, Y. Kim, T.-I. Lee, I. Lee, J. Shin, H. S. Lee, T.-S. Kim, J. W. Choi, ACS nano 2015, 9, 12214.
- [12] I. Nam, G.-P. Kim, S. Park, J. W. Han, J. Yi, Energy & Environmental Science 2014, 7, 1095.
- [13] L. Liu, Y. Yu, C. Yan, K. Li, Z. Zheng, Nature communications 2015, 6, 1.
- [14] R. Xu, A. Hung, A. Zverev, C. Shen, L. Irie, G. Ding, M. Whitmeyer, L. Ren, B. Griffin, J. Melcher, "A Kirigami-inspired, extremely stretchable, high areal-coverage micro-supercapacitor patch", presented at *2018 IEEE Micro Electro Mechanical Systems (MEMS)*, 2018.
- [15] T. G. Yun, B. I. Hwang, D. Kim, S. Hyun, S. M. Han, ACS applied materials & interfaces 2015, 7, 9228.
- [16] H. Li, Z. Liu, G. Liang, Y. Huang, Y. Huang, M. Zhu, Z. Pei, Q. Xue, Z. Tang, Y. Wang, ACS nano 2018, 12, 3140.
- [17] R. Kumar, J. Shin, L. Yin, J. M. You, Y. S. Meng, J. Wang, Advanced Energy Materials 2017, 7, 1602096.
- [18] Z. Song, T. Ma, R. Tang, Q. Cheng, X. Wang, D. Krishnaraju, R. Panat, C. K. Chan, H. Yu, H. Jiang, Nature communications 2014, 5, 1.
- [19] W. Liu, J. Chen, Z. Chen, K. Liu, G. Zhou, Y. Sun, M. S. Song, Z. Bao, Y. Cui, Advanced Energy Materials 2017, 7, 1701076.
- [20] Y. Zhang, W. Bai, J. Ren, W. Weng, H. Lin, Z. Zhang, H. Peng, Journal of Materials Chemistry A 2014, 2, 11054.
- [21] J. Ren, Y. Zhang, W. Bai, X. Chen, Z. Zhang, X. Fang, W. Weng, Y. Wang, H. Peng, Angewandte Chemie 2014, 126, 7998.
- [22] Y. Zhang, W. Bai, X. Cheng, J. Ren, W. Weng, P. Chen, X. Fang, Z. Zhang, H. Peng, Angewandte Chemie International Edition 2014, 53, 14564.
- [23] L. Wang, Y. Zhang, J. Pan, H. Peng, Journal of Materials Chemistry A 2016, 4, 13419.
- [24] Y. Xu, Y. Zhao, J. Ren, Y. Zhang, H. Peng, Angewandte Chemie 2016, 128, 8111.
- [25] H. Li, Y. Ding, H. Ha, Y. Shi, L. Peng, X. Zhang, C. J. Ellison, G. Yu, Advanced Materials 2017, 29, 1700898.